Mapping Swamp Timothy *(Cripsis schenoides)* Seed Productivity Using Spectral Values and Vegetation Indices in Managed Wetlands

Patrick Rahilly[1,2]*, Donghai Li[1], Qinghua Guo[1], Jinxia Zhu[1], Ricardo Ortega[2], Nigel W.T. Quinn[3], and Thomas C. Harmon[1]

[1]School of Engineering and Sierra Nevada Research Institute
University of California, Merced
[2]Grasslands Water District
[3]HydroEcological Engineering Advanced Decision Support
Lawrence Berkeley National Laboratory

May 1, 2009

*Corresponding Author: Patrick Rahilly, School of Engineering, University of California, Merced, Merced, CA 95344, Email: prahilly@ucmerced.edu, Ph: 209.761.0753

Mapping Swamp Timothy *(Cripsis schenoides)* Seed Productivity Using Spectral Values and Vegetation Indices in Managed Wetlands

Abstract

This work examines the potential to predict the seed productivity of a key wetland plant species using spectral reflectance values and spectral vegetation indices. Specifically, the seed productivity of swamp timothy *(Cripsis schenoides)* was investigated in two wetland ponds, managed for waterfowl habitat, in California's San Joaquin Valley. Spectral reflectance values were obtained and associated spectral vegetation indices (SVI) calculated from two sets of high resolution aerial images (May 11, 2006 and June 9, 2006) and were compared to the collected vegetation data. Vegetation data were collected and analyzed from 156 plots for total aboveground biomass, total aboveground swamp timothy biomass, and total swamp timothy seed biomass. The SVI investigated included the Simple Ratio (SR), Normalized Difference Vegetation Index (NDVI), Soil Adjusted Vegetation Index (SAVI), Transformed Soil Adjusted Vegetation Index (TSAVI), Modified Soil Adjusted Vegetation Index (MSAVI), and Global Environment Monitoring Index (GEMI). We evaluated the correlation of the various SVI with in situ vegetation measurements for linear, quadratic, exponential and power functions. In all cases, the June image provided better predictive capacity relative to May, a result that underscores the importance of timing imagery to coincide with more favorable vegetation maturity. The north pond with the June image using SR and the exponential function (R^2=0.603) proved to be the best predictor of swamp timothy seed productivity. The June image for the south pond was less predictive, with TSAVI and the exponential function providing the best correlation (R^2=0.448). This result was attributed to insufficient vegetal cover in the south pond (or a higher percentage of bare soil) due to poor drainage conditions which resulted in a delay in swamp timothy germination. The results of this work suggest that spectral reflectance can be used to estimate seed productivity in managed seasonal wetlands.

1 Introduction

Prior to 1850, there were an estimated 5 million acres of wetlands in California. Today, less than 6% remain (Hartmann 1994). The remaining wetlands are now intensively managed to provide habitat for 19% of the wintering waterfowl in the continental U.S. and 60% of the waterfowl of the Pacific Flyway (Gilmer *et al.*, 1982). In 1986, The North American Waterfowl Management Plan was drafted by the U.S. Fish and Wildlife Service in cooperation with Canadian Wildlife Service. A goal of this plan is to increase waterfowl populations to their pre-1970 numbers "by improving and securing long-term protection of 6 million acres of habitat [nationally] in 34 areas of major concern" (USFWS 1986). Wetland health and productivity greatly affects waterfowl populations (Fleskes et al. 2005, Mushet *et al* 1992). Wetland managers are striving to provide habitat support to accommodate growing populations of waterfowl.

The wetlands in California's Central Valley are managed by controlled flooding in the late summer, maintaining water levels through the winter, and then draining in the spring (Fredrickson and Taylor 1982, Naylor 1999). The timing and rate of spring drawdown affect

many aspects of habitat health including vegetation composition. The varieties of annual plants that geminate on the exposed mudflats of the seasonal wetlands after water is drained are collectively known as moist-soil plants. The seeds and tubers produced by moist-soil plants during these summer months feed the wintering waterfowl. Soil moisture, soil salinity, and both soil and air temperatures at time of germination are affected by timing and rate of drawdown and directly affect the overall moist-soil plant species composition (Naylor 1999).

Swamp timothy (*Cripsis schenoides*) is one of the key forage species in managed wetlands of the Central Valley (Fleskes et al. 2004 and 2005). It is a fast-growing annual producing high quality seeds in great quantities. It is tolerant of both temporary inundation induced by summer irrigation and moderate to high soil salinity levels inherent in Central California wetland soils (Fredrickson and Taylor 1982, Mushet et al. 1992). Bird species that forage on swamp timothy seeds are primarily ducks such as pintails, gadwalls, mallards, and teal (Hothem and Ohlendorf 1989, Fleskes et al. 2004 and 2005, Burns et al. 2003). Wetlands managed for swamp timothy are also utilized by many shorebird species such as dunlins, sandpipers, and the American avocet due to its low growth habit (Isola et al. 2000). A challenge facing wetland managers is to efficiently quantify the amount of seed mass produced annually. Current techniques are both field and lab intensive and include manual biomass harvesting and sorting of tiny seeds. Furthermore, because these labor-intensive methods can only be applied to representative vegetation stands within large wetland areas, they are prone to bias. Remote sensing techniques have the potential to enable large-scale assessment of feed biomass in this wildland setting.

It is well documented that digital spectral reflectance values, as well as vegetation indices derived from these spectral values, can be used to estimate the total aboveground biomass produced on an annual basis (Asrar 1989, Jenson 2007). These techniques have been used to estimate crop yields (Richardson 1982, Moran et al. 1997, Godwin et al. 2003, Tao et al. 2005) and to quantify the areal extent of standing biomass in rangeland ecosystems (Everitt et al. 1989, Loris and Damiano 2006, Beeri et al. 2007, Cho et al. 2007). Moreau et al. 2003 used this technique to successfully estimate the areal extent of Andean wetland forage grasses. However, no one has assessed the potential of this technique to estimate annual seed mass production in a managed season wetland.

In our study which comprised pairs of managed wetland ponds, spatial vegetation data were collected and analyzed for total aboveground biomass, total aboveground swamp timothy biomass, and total swamp timothy seed mass. Our working hypothesis is that there is a strong correlation between the total swamp timothy biomass and seed mass. Assuming this to be true, the objective of this study is to assess the feasibility of using spectral reflectance values (red, and NIR bands) and their derived vegetation indices to estimate swamp timothy seed productivity. The analysis here is based on two sets of aerial imagery taken at different times approximately 4 weeks apart after pond drawdown in the adjacent wetland units, and on manually collected plant and seed biomass samples for the units.

2 Site Description and Methods

2.1 Site Description

An adjacent pair of privately owned wetland ponds within the Ducky Strike Duck Club, known as Ducky Strike North (DSN) and South (DSS), was chosen for this project because these ponds are dominated by swamp timothy (Figure 1). The ponds are located in the south-west part

of Merced County, California (south of 37°0′0″N and east of 12°50′0″W) within the Grasslands Ecological Area (GEA). The areas of DSN and DSS are 32.2 ha and 36.5 ha, respectively. Mean annual precipitation is 21cm and the mean annual temperature is 16.8°C (WRCC 2006). The soil series underlying the sites is Britto clay loam, ponded, derived from mixed alluvium dominantly of ocean sediments. Some of the chemical elements of this series include 5% maximum calcium carbonate, 10% gypsum, electric conductivity of 1.0 to 11.0 dS/m, sodium adsorption ratio maximum of 30.0, and pH values ranging from 6.0 to 8.5 (NRCS 2007). As noted above, this area is no longer naturally flooded but now diked and levied for controlled flooding typically lasting from the first of September to the middle of March. Within the DSN pond, the water flows from south to north following a swale located along the eastern edge of the field. DSS utilizes one inlet at the northeast corner of the field. The fields both slope gradually from west to east. Vegetation consists of swamp timothy, *Rumex spp*., *Eleocharis spp*., *Scirpus maritimus, Scirpus acutus, Juncus balticus, Typha spp.*, and *Xanthium strumarium* as the major components. The site is primarily managed for swamp timothy and often the emergent vegetation (rushes, tules, and cattails) are disked under to maintain maximum swamp timothy productivity while leaving some emergent vegetation for wildlife cover.

2.2 Aerial Imagery

False color composite high resolution aerial photographs were taken using a Zeiss RMK® Top 15 Aerial Survey Camera System on May 11 and June 9, 2006 (Figure 1). Images were taken at noon, zero degrees off nadir to minimize shadow effects. Missions were flown and imagery geo-rectified by HJW Geo-Spatial Inc. (Oakland, Ca). Ground pixel resolution is 15cm x 15cm (maximum RMS error 7.5cm). The coordinate system used for the images is UTM zone 10, NAD 83. Aerial images responded to green (G, 500-700 nm, red (R, 600-700 nm), and very near infrared (VNIR, 700-900 nm) spectral bands. The scanner produced RGB digital images with 8-bit false color with pixels in each band ranging from 0 to 255.

Calculations of vegetation indices are primarily based on reflectance while the aerial photographs record brightness. Therefore, radiation readings need to be corrected in order to determine the actual reflectance values of the imagery. As ground reflectance measurements were not made in 2006, a campaign was conducted in the study area in October 2008. Ground reflectance data was collected using a field spectrometer (ASD FieldSpec Pro FR) with a spectral range of 350 to 2500 nm. We collected spectra from 12 invariant targets (concrete and gravel surfaces) around the wetland ponds. The reflectance of 12 targets at green, red, near infrared bands exhibited a highly linear correlation ($R^2 > 0.95$) with brightness. Because reflectance from these surfaces is not expected to change with time, we used these results to correct the 2006 aerial images, yielding the reflectance products used in subsequent analyses.

2.3 Vegetation Sampling and processing

Vegetation sampling was conducted in August of 2006 after the swamp timothy seeds had matured and the entire plant was desiccated. Sampling granularity was one 1m x 1m sampling location per acre (DSS n=73, DSN n=83), with each location randomly generated using GIS software (ArcGIS 9.3, ESRI). A Trimble Ag114 GPS receiver connected to a hand held PC (Allegro Cx, Juniper Systems) with determined 15cm accuracy was used to locate each sampling location. At each location, a representative 10cm x 10cm core was removed from the pedon, allowing the entire aboveground biomass to be clipped. Samples were oven-dried at 105°C for

24 hours. Dry masses of total biomass, total swamp timothy, and swamp timothy seeds were determined gravimetrically for each sample.

2.4 Spectral Reflectance and Vegetation Indices

In this study, we tested the feasibility of two spectral reflectance bands (red and near infrared) and six vegetation indices as predictors of swamp timothy seed production. Vegetation indices for quantifying biomass or vegetative vigor were derived from spectral bands, and were broadly separated into three categories: 1) intrinsic indices such as the simple ratio (Jordan 1969, Baret and Guyot 1991) and the NDVI (Kriegler et al.1969, Rouse et al. 1974) which does not involve any external factor other than the measured spectral reflectance; 2) soil-line related indices, which include soil-line parameters, such as the soil-adjusted vegetation index or SAVI (Huete 1988), the transformed SAVI (Baret 1989), and the modified SAVI (Qi et al., 1994); and 3) atmospheric-corrected indices such as GEMI (Pinty 1992). Mathematical descriptions of the indices are summarized in Table 1.

The spectral reflectance of a plant canopy is a combination of the reflectance spectra of plant and soil components. A linear relationship between the red and near infrared reflectance on bare soil (the soil line) can be developed from base soil areas at a site and incorporated into vegetation indices to reduce the influence of the soil on the vegetation response (Genevieve 1996). In this research, the soil line used to calculate the TSAVI was obtained by randomly selecting 113 and 104 bare soil pixels from the May and June imagery, respectively, and using these pixels to develop a regression between the red and near infrared band reflectance values.

2.5 Statistical Analysis and Creating Swamp Timothy Productivity Maps

To accurately analyze relationships between seed mass with spectral reflectance and vegetation indices, the cell size of the spectral reflectance and vegetation indices must be consistent with the $1m^2$ field sample scale. Specifically, the cell size was altered to 7 by 7 pixels around each sample coordinate (equaling 1.05 m^2, approximately equal to the field sample area). The VNIR and red pixel reflectance values for each cell were then averaged and used to calculate the vegetation indices are in Table 1.

The relationship between vegetation index and biophysical variables has been modeled using a variety of mathematic functions: linear, exponential, power, quadratic, and logarithm terms (Lewis et al. 1998, Rasmussen 1992, Groten 1993, Pinter et al. 1981, Thenkabail et al. 1994). These models were tested with a regression analysis of spectral reflectance and vegetation indices with swamp timothy biomass and seed biomass (Pinter et al. 1981, Rasmussen 1992, Groten 1993, Thenkabail et al. 1994, Lewis et al. 1998). Determination coefficients (R^2) were estimated using SPSS 16.0 (SPSS inc.) and used to differentiate model quality.

To create swamp timothy seed mass maps, the best predictive models were used to assign swamp timothy seed mass to each 7 by 7 pixel. Because the DSN and DSS ponds are not entirely swamp timothy inclusive habitat, those non-swamp timothy areas were eliminated from the map using a classification by a segmentation technique in eCognition,v2.0 (Definiens Inc.).

3 Results

Swamp timothy total biomass correlated strongly with swamp timothy seed mass (R^2 = 0.856) in the DSN pond and moderately (R^2 = 0.653) in DSS (Figure 2), validating our working hypothesis and suggesting that swamp timothy seed production can be accurately estimated

across a broad landscape using spectral values and vegetation indices. Coefficients of determination for all models tested are summarized in Table 2, and the best-fitting models for seed production are plotted in Figure 3.

Overall, the best swamp timothy seed mass predictions were obtained using the DSN June image with the greatest values achieved using SR (R^2 = 0.603), NDVI (0.581), and TSAVI (0.581) in exponential, exponential, and quadratic models, respectively. Red (quadratic) SAVI (quadratic) and MSAVI (exponential) models yielded comparable but lower coefficients, while the GEMI and NIR model fits were inferior. The Red band produced results that were consistently better than NIR. In four of the six indices investigated, the exponential model outperformed the other models tested with the June DSN image. Both May images and the June DSS image resulted in poorer seed production predictions in all cases. In the case of June DSS, the same three indices--SR, NDVI, and TSAVI--were the top predictors, albeit weaker ones relative to the June DSN results.

In most cases, total biomass and total swamp timothy biomasses (primary properties) produced better model fits than did swamp timothy seed mass (secondary property). NDVI, SR, SAVI, TSAVI, MSAVI, and Red were found to be relatively good indicators for these properties, while again GEMI and NIR were found to be relatively weak indicators.

Models resulting from the May images, and from the DSS June image, generally performed poorly relative to those obtained from the June DSN image. The exception was the total biomass model obtained from the May DSN image, which yielded determination coefficient values comparable to those obtained using the June DSN image.

The swamp timothy seed productivity map (Figure 4) was created using the best vegetation index and June image for each pond. The areas of the wetland units with relatively high swamp timothy seed productivity match the areas with lower soil salinity and the lower elevation areas of the fields (Rahilly 2008). An overall trend observed with respect to swamp timothy seed production is for greater abundance in the east portion of the field relative to the the west . The southern portions of both fields contain relatively little swamp timothy. Note that the areas mapped in red indicate portions of the field that were determined to be non-inclusive swamp timothy habitat (e.g. tules, cattails, and Baltic rush).

4 Discussion

The SR from the June DSN image exhibited moderately strong correlation with seed productivity (R^2=0.603). This is a reasonable result considering within-field variability at the study sites, where soil moisture, salinity, and vegetative composition all vary across the landscape. For example, moist soil plant growth on the east side of DSN was significantly greater than on the west side, and sufficiently high to cause saturation of the NDVI (Mutanga and Skidmore 2004, Loris and Damiano 2006, Jenson 2007) and the other spectral signatures. According to Muntanga and Skidmore (2004), this saturation problem can be overcome by using a narrow band NDVI (740nm – 755nm). Unfortunately, this was not possible with our imagery because the NIR band in our imagery was an average of 700-900 nm, an artifact of the camera used.

Results for DSS seed productivity were inferior to those for DSN, This result is A finding consistent with the fact that total aboveground biomass and swamp timothy seed mass is not as strong in DSS as it was in DSN. This suggests that although the two ponds are adjacent, there are inherent differences between their soils which translated to differences in swamp

timothy seed production.. Based on EM surveys from the site, the apparent soil salinity in DSS is greater than that in DSN (Rahilly 2008). Elevated salinity in DSS is most likely associated with less effective drainage in this pond due to isolated topographic depressions in the pond (Rahilly 2008). In addition, the same hydraulic structure is employed for both flooding and draining in DSS, a situation which may contribute to its drainage inefficiencies. The NIR band image of the two ponds (Figure 1) illustrates the poor and prolonged drainage time of DSS compared to DSN. The dark spots in DSS May image are exposed mudflats where the annual plants have not yet begun to germinate. In comparison, DSN exhibits vegetation across the entire field at this time. While swamp timothy eventually germinates in DSS, the end result is less growth, probably due to the stressful growing conditions relative to those experienced in DSN . The more stressful growing conditions in DSS would force the swamp timothy to focus its energy on seed production rather than biomass production which may explain the weaker correlation between total swamp timothy biomass and seed biomass in DSS.

Several issues with respect to the timing of sampling events in our investigation merit further discussion. First, our clip samples were collected in August 2006, nearly two months after the June aerial imagery event and at a time when the vegetation was desiccated. While this timing greatly facilitated seed collection, it precluded the preferred usage of wet over dried biomass in relating vegetation indices to productivity (Tucker, 1983). A second and more crucial issue pertains to the timing of the aerial photography. By the time of the June imagery, the vegetation in DSS and DSN was highly stressed and wilting. This is evidenced by the fact that the red spectral reflectance band exhibited better correlation than the VNIR band in these images (Table 2), a finding in accord with Jenson (2007). The correlations resulting from this work may have been stronger had the photography occurred before the onset of wilting. Of course, if the images are taken too early in the season, the results will suffer from lack of vegetation cover resulting in high soil reflectance, as was the case with the May results. Thus, it is clear that more research is warranted with respect to the optimal imagery timing for this type of investigation..

In field locations where vegetation is homogeneous, relationships between vegetation indices and biomass have produced satisfactory results (Frank and Aase 1994). However, if plant communities are diverse, additional vegetation information about community structure may need to be collected. In this context, it is worth noting that there may have been vegetation-specific causes for elevated red reflectance in the June imagery. Specifically, *Rumex spp.*, a common species that grows in these fields, is bright rust red in color, and may bias the reflectance values by overwhelming the influence of the green chlorophylls. Where there are different chlorophyll and carotenoids, such as may be found with *Rumex,* the use of the green band instead of the red band when calculating NDVI or SR may produce better results (Gitelson et al. 1996; Loris et al. 2006).

While it has been noted that SR-based correlations with crop yield outperform NDVI-based models (Mutanga and Skidmore, 2004), less has been written about mixed vegetation. Both of the DSN images resulted in stronger correlations between the intrinsic (as opposed to the soil-adjusted) vegetation indices and swamp timothy seed production. This was particularly the true for the May image although, as noted, all of the determination coefficients associated with seed production were relatively lower for May. In both the May and June DSN results, the SR model outperformed the NDVI model. In a somewhat related study, Loris and coworkers (2006) reported that SR was best for estimating meadow grass productivity from aerial imagery. Meadow grass is typically a diverse array of grasses and forbs, analogous in structure to the present wetland moist-soil plant community.

5 Conclusions

The results of this study suggest that the use of spectral reflectance-based vegetative indices to predict swamp timothy seed productivity in seasonally managed wetlands setting is feasible. Accuracy of the resulting model depends on coordination of the imaging with the key management event (draw-down), which in turn triggers changes in the drivers in swamp timothy production, namely soil moisture, temperature and salt accumulation. The results suggest that a less intensive field sampling effort can be utilized to calibrate a model in order to create swamp timothy biomass and seed productivity maps. Methods for more efficient assessment of wetland seed productivity will enable wetland managers to adaptively manage the wetlands in support of waterfowl.

Acknowledgments

Funding for this work was provided by the State Water Resources Control Board (Grant # 04-312-555-1, the University of California Salinity Drainage Program and the California Department of Water Resources. This work was also partially supported by the U.S. Department of Energy and LBNL under Contract No. DE-AC02-05CH11231.

6 Literature Cited

Anderson, G. L., J. D. Hanson, R. H. Haas. 1993. Evaluating Landsat Thematic Mapper derived vegetation indices for estimating above-ground biomass on semiarid rangelands. Remote Sensing of Environment. 45:165-175.

Asrar, G. (editor). 1989. Theory and applications of optical remote sensing. John Wiley & Sons, Inc. New York.

Baret, F., G Guyot, and D Major. 1989. TSAVI: a vegetation index which minimizes soil brightness effects on LAI and APAR estimation, In: 12th Canadian Symposium on Remote Sensing and IGARSS '90, Vancouver, Canada, 10–14 July, 1989, pp. 1355–1358.

Baret, F. and G. Guyot. 1991. Potentials and limits of vegetation indices for LAI and APAR assessment. Remote Sensing of Environment, 35:161– 173.

Beeri, Ofer, Rebecca Phillips, John Hendrickson, Albert B. Frank, and Scott Kronberg. 2007. Estimating forage quantity and quality using aerial hyperspectral imagery for northern mixed-grass prairie. Remote Sensing of Environment 110:216-225

Burns, Ed, Michael Miller, and John Eadie. 2003. An analysis of Food Habits of Green-Winged Teal, Northern Pintails, and Mallards Wintering in the Suisun Marsh to Develop Guidelines for Food Plant Management. *A Report to the California Department of Water Resources and the United States Bureau of Reclamation*.

Chang, Jiyul, David E. Clay, Kevin Dalsted, Sharon Clay, and Mary O'Neill. 2003. Corn (*Zea mays L.*) yield prediction using multispectral and multidate reflectance. *Agronomy*. 95:1447-1453.

Cho, Moses Azong, Andrew Skidmore, Fabio Corsi, Sipke E. van Wieren, and Istiak Sobhan. 2007. Estimation of green grass/herb biomass and partial least squares regression. International Journal of Applied Earth Observaion and Geoinformation 9:414-424

Everitt, J.H., D.E. Escobar, A.J. Richardson. 1989. Estimating grassland phytomass production with near-infrared and mid-infrared spectral variables. Remote Sensing of Environment 30:257-261.

El-Haddad, El-Sayed H. and Maher M. Noaman. 2001. Leaching Requirement and Salinity threshold for the Yield and Agronomic Characteristics of Halophytes Under Salt Stress. *Journal of Arid Environments* 49: 865-874.

Fleskes, Joseph P., David S. Gilmer, and Robert L. Jarvis. 2004. Habitat Selection by Female Northern Pintails Wintering in the Grassland Ecological Area, Califonia. *California Fish and Game* 90 (1): 13-28.

Fleskes, Joseph P., David S. Gilmer, and Robert L. Jarvis. 2005. Pintail Distribution and Selection of Marsh Types at Mendota Wildlife Area During Fall and Winter. *California Fish and Game* 91 (4): 270-285.

Frank, A.B. and J.K. Aase. 1994. Residue effects on radiometric reflectance measurements of Northern Great Plains rangelands. Remote Sensing of Environment. 49:195-199.

Fredrickson, L.H. and T.S. Taylor. 1982. Management of Seasonally Flooded Impoundments for Wildlife. *Resource Publication #148*. U.S. Fish and Wildlife Service, Washington, DC, USA.

Gilmer, K.S., M.R. Miller, R.D. Bauer, and J.R. LeDonne. 1982. California's Central Valley wintering waterfowl: Concerns and challenges. *Transactions of the North American Wildlife and Natural Resource Conference* 47:441-452.

Gitelson, A.A., Y.J. Kaufman, and M.N. Merzlyak. 1996. Use of a green channel in remote sensing of global vegetation from EOS-MODIS. Remote Sens. Environ. 58: 289–298.

Godwin, R.J., G.A. Wood, J.C. Taylor, S.M. Knight, and J.P. Welsh. 2003. Precision farming of cereal crops: a review of a six year experiment to develop management guidelines. Biosystems Engineering 84(4): 375-391.

Groten S.M.E. 1993. NDVI—crop monitoring and early yield assessment of Burkina Faso. International Journal of Remote Sensing. 14:1495-1515.

Hartmann, Joan R., and Jon H. Goldstein. 1994. *California's Central Valley. Chapter XI*. The Impact of Federal Programs on Wetlands: A Report to Congress by the Secretary of the Interior *vol. II*. http://www.doi.gov/oepc/wetlands2/v2ch11.html. Revised: 07-09-96.

Hothem, Roger L. and Harry M. Ohlendorf. 1989. Contaminants in Foods of Aquatic Birds at Kesterson reservoir, California, 1985. Archives of Environmental Contamination and Toxicology 18: 773-786.

Huete, A.R., 1988. A soil adjusted vegetation index (SAVI). Remote Sensing of Environment 25: 295–309.

Isola, C.R., M.A. Colwell, O.W. Taft and R.J. Safran. 2000. Interspecific Differences in Habitat Use of Shorebirds and Waterfowl Foraging in Managed Wetlands of California's San Joaquin Valley. *Waterbirds* 23(2): 196-203.

Jenson, John R. 2007. *Remote Sensing of the Environment: An Earth Resource Perspective.* New Jersey: Pearson Prentice Hall.

Jordan, C.F. 1969. Derivation of leaf area index from quality of light on the forest floor. Ecology 50: 663–666.

Kriegler, F.J., W.A. Malila, R.F. Nalepka, W. Richardson. 1969. Preprocessing transformations and their effects on multispectral recognition. In: Proceedings of the 6th International Symposium on Remote Sensing of Environment, University of Michigan, Ann Arbor, MI, pp. 97–131.

Lewis, J.E., J. Rowland, and A. Nadeau. 1998. Estimating maize production in Kenya using NDVI: some statistical considerations. International Journal of Remote Sensing. 19(13), 2609-2617.

Loris, Vescovo and Gianelle Damiano. 2006. Mapping the green herbage ratio of grasslands using both aerial and satellite-derived spectral reflectance. Agriculture, Ecosystems and Environment 115:141-149.

Moran, M.S., Y. Inoue, E.M. Barns. 1997. Opportunities and limitations for image-based remote sensing in precision crop management. Remote Sensing of Environment 61:319-346.

Moreau, Sophie, Roland Bosseno, Xing Fa Gu, and Frederic Baret. 2003. Assessing the biomass dynamics of Andean *bofedal* and *totora* high-protein wetland grasses from NOAA/AVHRR. Remote Sensing of Environment 85:516-529.

Mushet, David M., Ned H. Euliss, Jr., and Stnaley W. Harris. 1992. Effects of Irrigation on seed Production and Vegetative characteristics of Four Moist-Soil Plants on impounded Wetlands of California. *Wetlands,* Vol. 12, No. 3. December, pp. 204-207.

Mutanga, O. and A.K. Skidmore. 2004. Narrow band vegetation indices overcome the saturation problem in biomass estimation. International Journal of Remote Sensing vol. 25, no. 19, 3999-4014.

Naylor, Luke W. 1999. *Thesis: Evaluating Moist-Soil Production and Management in Central Valley Wetlands to Determine Habitat Needs for Waterfowl*. University of California, Davis.

NRCS. 2007. Web Soil Survey. http://websoilsurvey.nrcs.usda.gov/app/ . USDA, NRCS. *last updated 6/20/2007: visited 12/10/2007.*

Pinter, P.J., R.D. Jackson, S,B, Idso, R.J. Reginato. 1981. Multidate spectral reflectance as predictors of yield in water stressed wheat and barley. International Journal of Remote Sensing, 2: 43 – 48

Pinty, B., and M.M. Verstraete. 1992. GEMI: a non-linear index to monitor global vegetation from satellites. Vegetatio, 101: 15– 20.

Qadir, M., A. Ghafoor, and G. Murtaza. 2000. Amelioration Strategies for Saline Soils: A Review. *Land Degradation and Development* 11: 501-521.

Qi, J., A. Chehbouni, A.R. Huete, Y.H. Kerr, S. Sorooshian. 1994. A modified soil adjusted vegetation index. Remote Sensing of Environment 48, 119–126.

Rahilly, Patrick J.A. 2008. *Thesis: Investigating the dynamics of managed wetland ecosystems in the Grasslands Ecological Area, Merced County, Ca.* University of California, Merced.

Rao, B.R.M., T. Ravi Sankar, R. S. Dwivedi, S. S. Thammappa, L. Venkataratnam, R. C. Sharma, and S. N. Das. 1995. Spectral behavior of salt-affected soils. International Journal of Remote Sensing 16: 2125-2136.

Rasmussen, M.S. 1992. Assessment of millet yields and production in northern Burkina Faso using integrated NDVI from the AVHRR. International Journal of Remote Sensing. 13(18): 3431 - 3442

Richardson, A.J., C.L. Wiegand, G.F. Arkin, P.R. Nixon, and A.H. Gerbermann. 1982. Remotely-sensed spectral indicators of sorghum development and their use in growth modeling. Agricultural Meteorology, 26:11-23.

Rouse, J.W., R.H. Hass, J.A. Shell, and D.W. Deering. 1974. Monitoring vegetation systems in the great plains with ERTS-1. In: Proceedings 3rd Earth Resources Technology Satellite Symposium, vol. 1. pp. 309–317.

Thenkabail, P.S., A.D. Ward, and J.G. Lyon. 1994. Landsat-5 Thematic Mapper models of soybean and corn crop characteristics. International Journal of Remote Sensing, 15: 49 – 61.

Thenkabail, P. S. 2003. Biophysical and yield information for precision farming from near-real-time and historical Landsat TM images, International Journal of Remote Sensing, 24:14,2879 — 2904

Toa, Fulu, Masayuki Yokozawa, Zhao Zhang, Yinlong Xu, and Yousay Hayashi. 2005. Remote Sensing of Crop Production in China by Production Efficiency Models: Models Comprisons, Estimates and Uncertainities. *Ecological Modelling* 183: 385-396.

Tucker, C.J. 1983. Satellite remote sensing of total dry matter production in the Senegalese Sahel. Remote Sensing of Environment 13:461-474.

U.S. Fish and Wildlife Service. 1986. North American Waterfowl Management Plan. *U.S. Fish and Wildlife Service, Portland, Or*.

Western Region Climate Center (WRCC). 2006. http://www.wrcc.dri.edu/cgi-bin/cliGCStT.pl?calosb. WRCC. wrcc@dri.edu. *Last updated 7/28/2006: visited 12/10/2007.*

Wylie, B.K., D.J. Meyer, L.L. Tieszen, and S. Mannel. 2002. Satellite mapping of surface biophysical parameters at the biome scale over the North American grasslands: A case study. Remote Sensing of Environment 79:266-278.

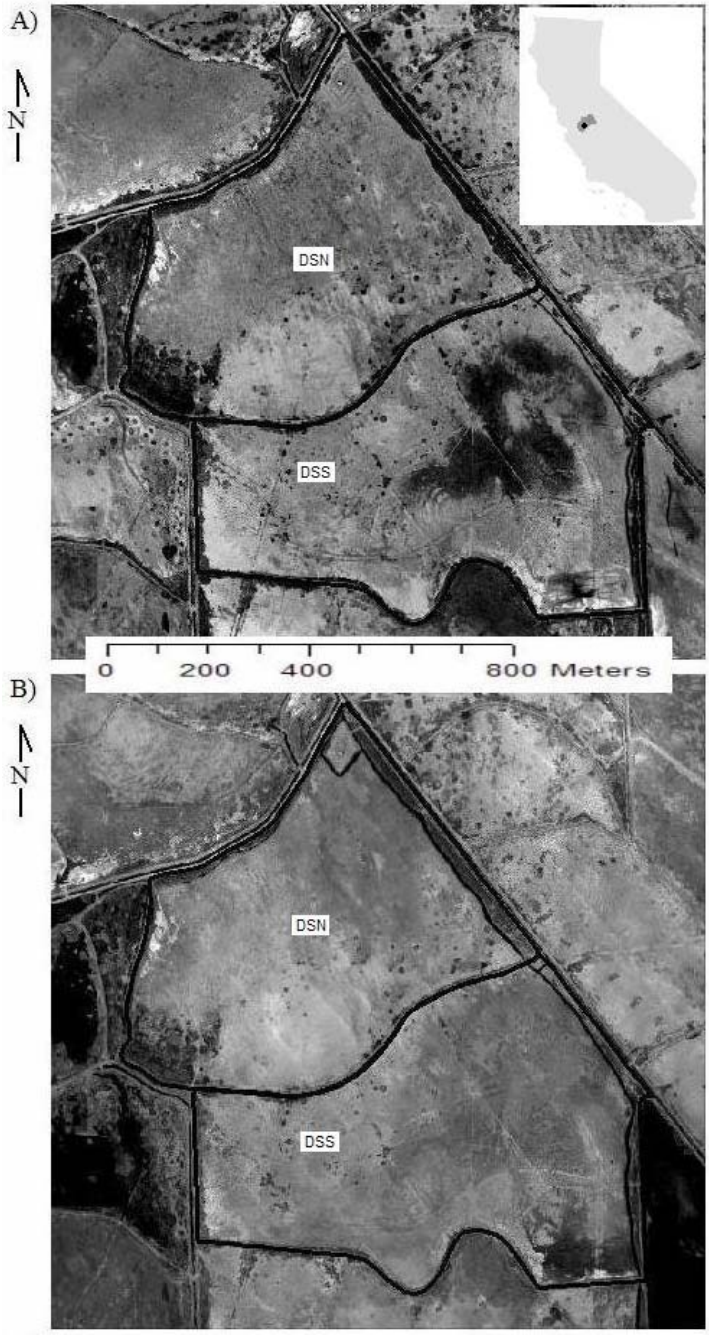

Fig. 1 Ducky Strike North (DSN) and Ducky Strike South (DSS): NIR spectral reflectance band; A) May 11,2006; B) June 9,2006.

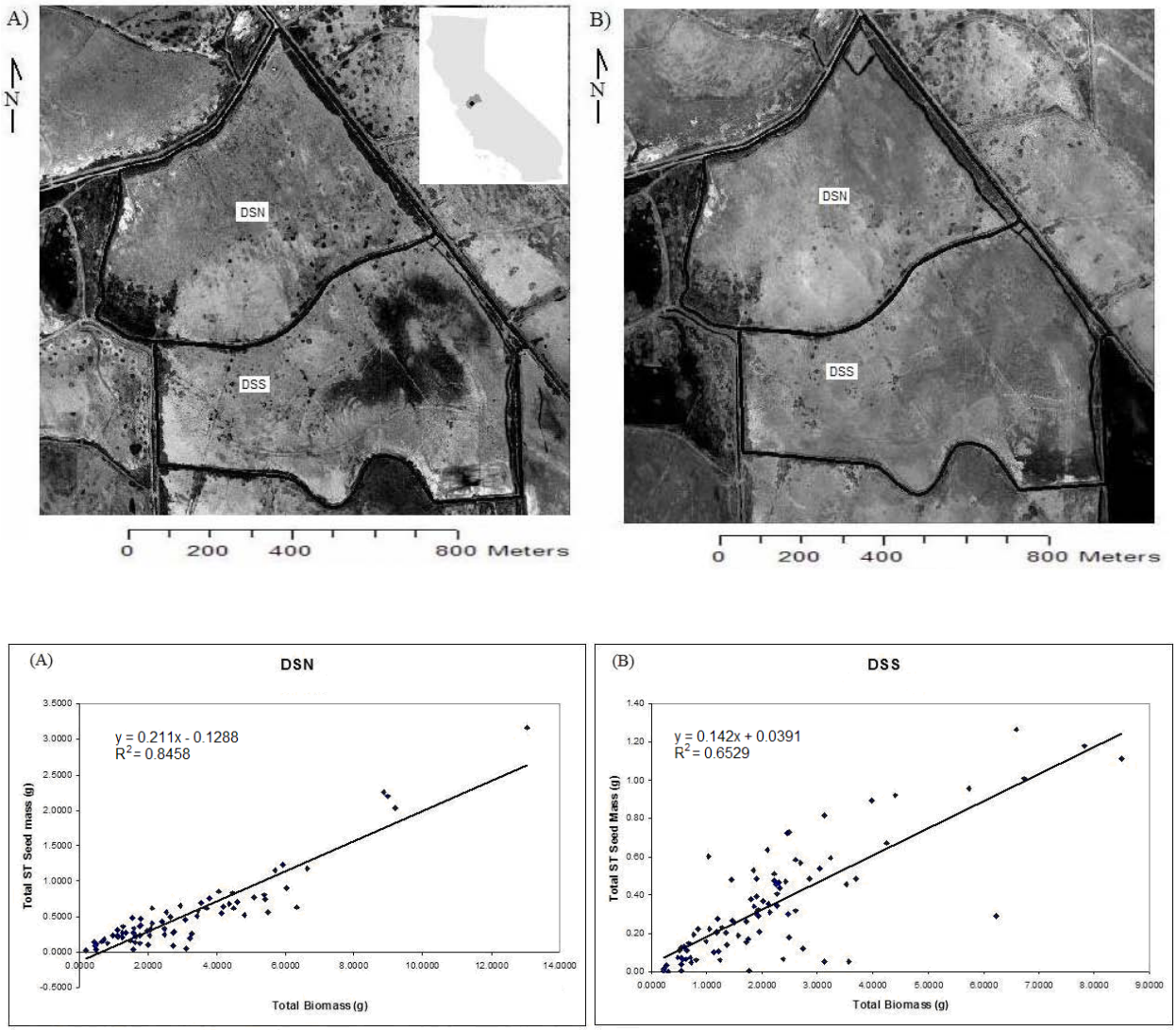

Fig. 2 Total aboveground biomass (grams) to swamp timothy (ST) seed mass (grams). Ducky Strike North, (B) Ducky Strike South.

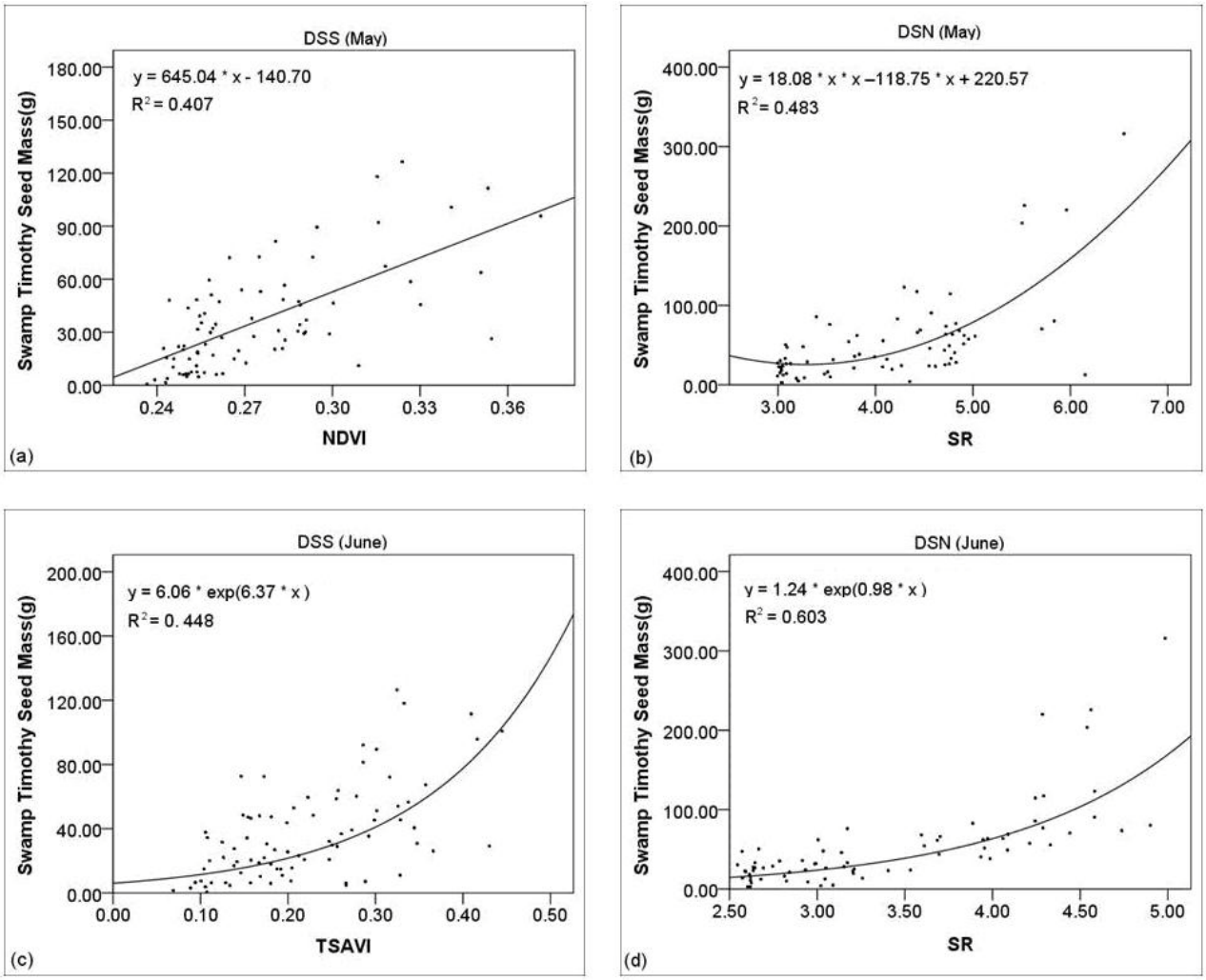

Fig. 3 Observed swamp timothy seed mass(g/m^2) plotted to the best correlated vegetation indices in two fields, Ducky Strike North (DSN) and Ducky Strike South (DSS) from aerial photos taken on two different dates (May 11,2006 and June 9,2006).

Table 1 Vegetation indices used in this study

Vegetation Index Name	Abbreviation	Description	Reference
Normalized difference vegetation index	NDVI	$NDVI = \frac{\rho_{nir} - \rho_{red}}{\rho_{nir} + \rho_{red}}$, where ρ_{red} and ρ_{nir} stand for the spectral reflectance measurements acquired in the red and near-infrared regions, respectively.	Rouse et al. 1974, Kriegler et al. 1969
Simple ratio	SR	$SR = \frac{\rho_{nir}}{\rho_{red}}$, Near-infrared/Red reflectance ratio.	Baret and Guyot 1991 Jordan 1969
Soil-adjusted vegetation index	SAVI	$SAVI = \frac{(1+L)*(NIR-R)}{NIR+R+L}$ L ranges from 0 for very high vegetation cover to 1 for very low vegetation cover. L=0.5 is used in this study.	Huete 1988
Transformed soil-adjusted vegetation index	TSAVI	$TSAVI = \frac{a \cdot (\rho_{nir} - a \cdot \rho_{red} - b)}{\rho_{red} + a \cdot \rho_{nir} - a \cdot b}$ Where a and b are, respectively, the slope and the intercept of soil line* ($\rho_{nir} = a * \rho_{red} + b$)	Baret 1989
Modified soil-adjusted vegetation index	MSAVI	$MSAVI = \frac{(1+L)*(\rho_{nir} - \rho_{red})}{\rho_{nir} + \rho_{red} + L}, L = 1 - 2 * a * NDVI * WDVI, WDVI = \rho_{nir} - a * \rho_{red}$	Qi,et al. 1994
Global environment monitoring index	GEMI	$GEMI = \frac{\eta*(1-0.25*\eta) - (\rho_r - 0.125)}{1-\rho_{nir}}, \eta = \frac{[2(\rho_{nir}^2 - \rho_r^2) + 1.5*\rho_{nir} + 0.5*\rho_r]}{\rho_{nir} + \rho_r + 0.5}$ GEMI can reduce both the soil and the atmospheric effects on satellite data.	Pinty 1992

*Soil line models for this work based on site imagery for May: ρ_{nir} = 1.760(ρ_{red}) + 0.041 (R^2 = 0.792); and (June): ρ_{nir} = 1.742(ρ_{red}) + 0.083 (R^2 = 0.821).

Table 2 Ducky Strike (DS) R^2 of best fit regression lines for various biomass measurements (g/m^2) plotted against spectral reflectance and vegetation indices. L:Linar, Q:Quadratic, E:Exponential, P:Power

May:	**VNIR**	**Red**	**NDVI**	**SR**	**SAVI**	**TSAVI**	**MSAVI**	**GEMI**
DSN								
Total Biomass	0.269 ^{E}	0.580 ^{E}	0.613 ^{P}	0.622 ^{E}	0.501 ^{E}	0.608 ^{E}	0.457 ^{E}	0.214 ^{E}
Total ST	0.201 ^{Q}	0.404 ^{Q}	0.405 ^{Q}	0.469 ^{Q}	0.282 ^{Q}	0.399 ^{Q}	0.273 ^{Q}	<0.1
ST seed biomass	0.229 ^{Q}	0.404 ^{Q}	0.402 ^{Q}	0.483 ^{Q}	0.242 ^{E}	0.391 ^{Q}	0.235 ^{E}	<0.1
DSS								
Total Biomass	<0.1	0.335 ^{Q}	0.426 ^{L}	0.443 ^{E}	0.409 ^{Q}	0.401 ^{E}	0.406 ^{P}	0.388 ^{E}
Total ST	<0.1	0.317 ^{Q}	0.446 ^{L}	0.403 ^{Q}	0.436 ^{Q}	0.418 ^{Q}	0.438 ^{E}	<0.1
ST seed biomass	<0.1	0.316 ^{Q}	0.407 ^{L}	0.338 ^{L}	0.370 ^{Q}	0.378 ^{E}	0.372 ^{L}	<0.1
June:								
DSN								
Total Biomass	0.455 ^{E}	0.660 ^{E}	0.656 ^{Q}	0.676 ^{Q}	0.650 ^{P}	0.663 ^{P}	0.631 ^{E}	0.549 ^{E}
Total ST	0.375 ^{P}	0.649 ^{Q}	0.693 ^{E}	0.716 ^{E}	0.654 ^{E}	0.697 ^{E}	0.645 ^{Q}	0.482 ^{E}
ST seed biomass	0.321 ^{P}	0.537 ^{Q}	0.581 ^{E}	0.603 ^{E}	0.539 ^{Q}	0.581 ^{Q}	0.537 ^{E}	0.440 ^{E}
DSS								
Total Biomass	<0.1	0.304 ^{E}	0.441 ^{Q}	0.443 ^{Q}	0.459 ^{E}	0.426 ^{E}	0.275 ^{Q}	0.181 ^{Q}
Total ST	<0.1	0.329 ^{Q}	0.476 ^{L}	0.472 ^{L}	0.356 ^{Q}	0.465 ^{L}	0.488 ^{E}	0.201 ^{Q}
ST seed biomass	<0.1	0.309 ^{E}	0.407 ^{L}	0.421 ^{L}	0.344 ^{Q}	0.448 ^{E}	0.311 ^{Q}	0.202 ^{Q}

Figure 4. Swamp timothy seed production map for DSN and DSS wetland ponds based on the SR-seed biomass exponential model for the June imagery (see Table 2).